THE ASTROPHYSICAL JOURNAL, 354:201–210, 1990 May 1

ENCOUNTERS BETWEEN COMPACT STARS AND RED GIANTS IN DENSE STELLAR SYSTEMS

FREDERIC A. RASIO[1] AND STUART L. SHAPIRO[1,2]
Center for Radiophysics and Space Research, Cornell University
Received 1989 August 2; accepted 1989 November 6

ABSTRACT

We present the results of some representative N-body simulations of encounters between a red giant star and a compact object. We have performed a preliminary survey of a large number of such encounters, varying all relevant parameters over wide ranges. We give an overview of all the different possible outcomes that can be produced by the encounters. Our combined analytic and numerical treatment is very general, but we pay particular attention to those encounters which lead to the formation of a binary system. In particular, we discuss how the numerical data on individual encounters can be used to calculate the binary formation rate in globular clusters, and we argue that the usual simple estimates based on the tidal approximation can sometimes give incorrect results. We also discuss the calculation of probability distributions for the semimajor axes and eccentricities of the binaries that are formed, as a function of globular cluster parameters. We show that encounters with stars on the *subgiant* branch might very well lead to the formation of close binaries ($a \sim 1$ $R_\odot$) with large eccentricity, such as those recently reported in 47 Tuc and M15. In addition, the binaries resulting from encounters with stars on the red giant branch could be an important source of heating during the late stages of evolution of a globular cluster.

Subject headings: clusters: globular — stars: binaries — stars: late-type — stars: neutron — stars: stellar dynamics

I. INTRODUCTION

The variety of physical processes which may take place during an encounter between a compact object and an ordinary red giant star poses a very challenging problem for investigation. From a physical point of view, the problem involves three-dimensional hydrodynamics with self-gravity, possibly coupled to nuclear burning and radiative transfer. Even a qualitative overview of the process demands a broad survey of many physical regimes and parameters in order to identify all the possible outcomes of an encounter (here we use the term "encounter" to describe both distant *tidal encounters* and direct physical *collisions* between the red giant and compact star). Nonetheless, these encounters are widely believed to take place and to be of great importance in several different astrophysical contexts. At least two have received considerable attention recently: one is the formation of close binary systems in the cores of globular clusters (see, e.g., Verbunt 1988*b* for a review and references) and the other is the production of high-velocity gas clouds in the central regions of galaxies (see Livne and Tuchman 1988 for a discussion).

That stellar encounters between a compact stellar remnant and an ordinary, main-sequence or giant star may be responsible for producing X-ray binaries in globular clusters was originally proposed by Fabian, Pringle, and Rees (1975), and Sutantyo (1975). In the Fabian, Pringle, and Rees scenario, a tidally dissipative, two-body encounter between a compact object and an ordinary main-sequence star leads to the capture of the compact object into a binary. Sutantyo, on the other hand, proposed that the X-ray binaries could be the results of *direct collisions* between compact stars and giants. Many calculations of the Fabian, Pringle, and Rees mechanism have been performed (Press and Teukolsky 1977; Lee and Ostriker 1986; Giersz 1986, McMillan, McDermott, and Taam 1987). These calculations are all based on perturbation expansions in terms of the normal modes of oscillation of the stars, modeled by a polytrope. However, very few calculations of direct physical collisions between a normal star and a compact object have been attempted, and all of them have been very approximate. This fact results from the highly nonlinear nature of the interaction and the absence of sufficiently powerful computers and reliable numerical techniques for handling serious three-dimensional hydrodynamics.

Recently, the idea of invoking encounters between a red giant and a compact object has been revitalized in the context of formation scenerios for ultra–short period binaries, believed to consist of a white dwarf and a neutron star. The so-called low-mass X-ray binaries, as well as binary millisecond pulsars, belong to this category. Bailyn (1988), for example, modified the Fabian, Pringle, and Rees argument for the case of tidal capture of a neutron star by a red giant. He showed that for red giants, direct collisions are likely to be more important for capture than distant tidal encounters, because of the larger physical cross section. Similarly, Verbunt (1987, 1988*b*; see also Verbunt and Meylan 1989) used globular cluster data to estimate relative rates for different binary mechanisms and concludes that collisions between neutron stars and red giant or horizontal branch stars are the most efficient mechanism for the formation in globular clusters of binaries containing a neutron star and a white dwarf.

The two recently reported new detections of rather peculiar binary millisecond pulsars in globular clusters will, if confirmed, raise a number of further questions concerning the possible formation scenarios of such objects. The first of them, PSR 0021 − 72A in 47 Tuc (Ables *et al.* 1988), appears to have an extremely small orbit, with a projected semimajor axis $a_1 \sin i = 585$ km, while at the same time it has retained a

[1] Department of Physics, Cornell University.
[2] Department of Astronomy, Cornell University.

large eccentricity, $e \approx 0.33$. The second one, PSR 2127+11C in M15 (Anderson *et al.* 1989), has a more reasonable separation, with an orbital period of 8.2 hr, but it also appears to have retained a very large eccentricity (Wolszczan 1989). However, it is generally thought that when a binary is formed by a two-body encounter, dissipation must circularise the orbit. On the basis of this, Wijers (1989) rules out red giant/neutron star collisions as a possible formation mechanism for the binary in 47 Tuc and argues instead in favor of a more complicated three-body capture process.

The ejection of a giant star's envelope due to the penetration of a compact object has also been studied in the somewhat different context of the "common envelope phase" of binary evolution (see, e.g., Taam, Bodenheimer, and Ostriker 1978; Bodenheimer and Taam 1984; Livio and Soker 1988). This phase in the evolution of some binary systems, where a giant star and its low-mass companion coalesce, is believed to be responsible for the formation of some cataclysmic variables, double white dwarf systems (progenitors of Type I supernovae), as well as some low-mass X-ray binaries. Calculations of this process usually assume that the mass of the penetrating star (which may be a main-sequence star as well as a compact star) is small compared to the mass of the giant, and that the orbit is initially circular. In such cases, energy is dissipated very slowly, and the penetrating body may spiral in on a time scale much longer than the crossing time. For example, Taam, Bodenheimer, and Ostriker (1978) have studied the penetration of an orbiting 1 $M_\odot$ neutron star into a 16 $M_\odot$ supergiant companion. Using a spherically symmetric stellar evolution code, they followed the slow restructuring of the envelope due to the local deposition of energy and angular momentum along the neutron star's orbit. In the presumably much more common case where an encounter takes place between two stars of comparable masses, the evolution is expected to be dominated by global gravitational interactions which take place on a much shorter time scale (of the order of the crossing time), so that circularization may not occur. In this case, the interaction is clearly three-dimensional and cannot be studied with a restricted method.

Finally, the disruption of a red giant's envelope due to its penetration by a compact object has been proposed as a mechanism for producing the high-velocity gas clouds observed in the very central parts ($r < 1$ pc) of galaxies (Lacy, Townes, and Hollenbach 1982). A simplified description of the typical encounter there is as follows: First, the giant's degenerate core interacts gravitationally with a high-velocity compact object, thereby receiving a velocity increment large enough for it to escape from the potential well of the envelope. The material in the envelope is left unbound. In response, a shock front, generated near the center, propagates radially outward and disrupts the envelope. Livne and Tuchman (1988; see also Tuchman 1985) estimate an envelope mass ejection rate of about $10^{-3} \cdot M_\odot$ yr^{-1} with typical velocities of 30–100 km s^{-1}. These values appear to fit the observed features of the clouds (as described by Lacy *et al.* 1980 and Lacy, Townes, and Hollenbach 1982) very well.

This paper is organized as follows. In § II, we introduce the general theoretical framework for our long-term computational study of encounters between compact objects and red giants. In § III, we present the results of some preliminary numerical calculations based on N-body simulations. Finally, in § IV, we discuss these preliminary results and motivate the need for more accurate hydrodynamical simulations, which will be presented in a forthcoming publication (Rasio and Shapiro 1990).

II. THEORETICAL FRAMEWORK

a) *Possible Outcomes of a Compact Object/Red Giant Encounter*

We first delineate the possible outcomes of an encounter. Our discussion is based partly on isolated examples that have been reported in the literature, and partly on our own numerical simulations, presented below in § III.

Three basic nondimensional ratios determine the dynamics of the encounter. These are the compact star/red giant mass ratio m_c/m_G, the ratio b/R_G of the impact parameter to the giant's radius, and the ratio $v_r/\tilde{v}$ of the relative velocity at infinity to the characteristic internal velocity of the problem, $\tilde{v} \equiv (Gm_G/R_G)^{1/2}$ ($\approx$ sound speed in the red giant's envelope). Depending on the values taken by these three ratios, a wide variety of qualitatively different outcomes is possible. Only once these outcomes are assessed can one evaluate the various formation rates and the probability distributions for observable quantities such as binary separation and eccentricity or mass ejection velocities. This second phase of the analysis requires information of the physical environment in which the encounters take place: the distribution of relative velocities v_r and the physical parameters and total number densities of the participating stars.

A fundamental distinction can be made between those encounters which leave the compact star unbound and those which do not. A further distinction can be made according to whether or not the red giant's structure is significantly altered. Specifically, we can distinguish six kinds of outcomes, listed here roughly in order of decreasing impact parameter b, decreasing relative velocity v_r, or decreasing m_c/m_G:

1. The core receives only a small impulse and subsequently undergoes heavily damped oscillations inside the envelope. A small fraction of the envelope's mass is ejected. (This is the typical behavior when $b/R_G \lesssim 1$ and $v_r/\tilde{v} \gg 1$.)

2. The core receives a velocity increment large enough for it to escape from the envelope's potential well. The envelope, released from the gravitational binding to the core, is subsequently disrupted. ($b/R_G \ll 1$ and $v_r/\tilde{v} \gg 1$.)

3. In some cases, an exchange between the compact object and the giant's core takes place, and the giant's envelope is only weakly perturbed (this was first noticed by Livne and Tuchman 1988).

4. The envelope is tidally disrupted by its interaction with the compact object. Enough energy is dissipated so that the compact object becomes bound and gets captured by the core, forming a binary. Some fraction of the envelope's mass may be accreted by one or both components of the binary. ($b/R_G \sim 1$ and $v_r/\tilde{v} \sim 1$.)

5. The compact star penetrates the envelope without perturbing it significantly and slowly spirals in toward the core. The energy released by friction is redistributed, and part or all of the envelope's mass is lost. (This seems to happen only when $m_c/m_G \ll 1$, as in the case of the interaction between a 16 $M_\odot$ supergiant and a 1 $M_\odot$ neutron star studied by Taam, Bodenheimer and Ostriker 1978.)

6. The compact star spirals in even more slowly toward the core. The energy deposited locally along the compact star's orbit is efficiently transported outward in the envelope and gets radiated away, so that little or no mass ejection takes place (Taam, Bodenheimer, and Ostriker 1978).

b) Simple Analytical Estimates

It is useful to perform a few analytical estimates for some simple cases to develop some intuition of the physical processes and the approximate scaling behavior of the results. These estimates can, in addition, provide useful checks on numerical simulations.

i) *Tidal Capture in the Impulsive Approximation*

For distant encounters with sufficiently large impact parameter and relative velocity, the impulsive approximation can be used to estimate the maximum impact parameter $b_{\max}(v_r)$ for a passing compact object with relative velocity v_r to be tidally captured. This was the basis of the Fabian, Pringle, and Rees mechanism mentioned in § I above. However, no actual calculation of this mechanism for red giant stars has ever been done. This is because of the breakdown in the standard method of analysis (Press and Teukolsky 1977) when the stellar oscillation modes become strongly damped, as is the case in core-halo structures (see McMillan, McDermott, and Taam 1987).

In the absence of an exact calculation, one may use the following crude derivation, based on an analogy with the case of tidal interactions of stellar systems (see, e.g., Binney and Tremaine 1987). Let us represent the red giant by a central point mass $m_{\rm core}$ surrounded by an envelope of mass $m_{\rm env}$ and density profile

$$\rho_{\rm env}(r) = \frac{(3-n)m_{\rm env}}{4\pi R_G{}^3}\left(\frac{R_G}{r}\right)^n . \tag{1}$$

For typical red giant models, $n \approx 1$ (Tuchman, Sack, and Barkat 1978).

The energy dissipated into thermal heat during the encounter is calculated in the tidal approximation as (eq. 7–55 of Binney and Tremaine 1987)

$$\Delta E = \frac{4G^2 m_c{}^2 m_{\rm env}\langle r^2\rangle G}{3v_r{}^2 r_p^4} , \tag{2}$$

where r_p is the periastron distance, and $\langle r^2\rangle_G \equiv m_{\rm env}{}^{-1}\int (x^2+y^2)\rho_{\rm env}\, d^3r$. Capture occurs if $\Delta E > \mu v_r{}^2/2$, where μ is the reduced mass. This gives the critical periastron distance $r_{\rm pc}$ for capture, in nondimensional form, as

$$\frac{r_{\rm pc}}{R_G} = \left[\frac{8}{3}\frac{m_c}{m_G}\frac{m_{\rm env}}{m_G}(1+m_c/m_G)\frac{\langle r^2\rangle_G}{R_G^2}\right]^{1/4} \times \left(\frac{\tilde v}{v_r}\right). \tag{3}$$

For the density profile of equation (1), we have $\langle r^2\rangle_G = (2/3)(3-n)/(5-n)R_G{}^2$, so that when $m_c/m_G \approx 1$ and $n \approx 1$ the coefficient of $\tilde v/v_r$ in equation (3) is very close to unity. Taking into account gravitational focusing, we obtain the maximum impact parameter for capture as

$$\frac{b_{\max}}{R_G} = \left[1 + 2(1+m_c/m_G)\frac{R_G}{r_{\rm pc}}\frac{\tilde v^2}{v_r^2}\right]^{1/2} \times \left(\frac{r_{\rm pc}}{R_G}\right). \tag{4}$$

A similar analysis is presented by Spitzer (1987) for the case of tidal capture by polytropic stars. In this case, a comparison can be made between the results obtained in the impulsive approximation and those obtained by the more exact method of Press and Teukolsky (1977).[3] For $n = 3$ polytropes, the agreement is found to be best (i.e., the values found for the critical periastron distance for capture agree to within a factor of 2) when the relative velocity at infinity is largest (see Table 6.2 of Spitzer 1987). For small v_r, the impulsive approximation largely overestimates the critical periastron distance. The agreement also appears to get better as the polytropic index n increases, i.e., for more centrally condensed density profiles. However, we still expect equation (4) to provide only an upper limit on the actual value of $b_{\max}$.

ii) *The "Head-on" Case*

For small impact parameter encounters, when $b \ll R_G$, even rather large relative velocities can lead to significant damage to the giant and/or capture of the giant's core into a binary with the compact object. For such encounters, it may be justified again to use the impulsive approximation to derive some approximate analytical results.

In the impulsive approximation, each fluid element in the envelope receives a velocity increment of magnitude

$$|\delta v_{\rm env}(x)| = \frac{2Gm_c}{v_r}(x^2+y^2)^{-1/2} , \tag{5}$$

perpendicular to the compact object's trajectory along the z-axis. The energy dissipated during the encounter is then approximately given by

$$\Delta E_{\rm env} \equiv \int \frac{1}{2}|\delta v(x)|^2 \rho_{\rm env}(x) d^3x = \frac{(3-n)G^2 m_c{}^2 m_{\rm env}}{R_G{}^2 v_r{}^2} I_n\left(\frac{b_{\min}}{R_G}\right), \tag{6}$$

where the density profile of equation (1) has been used. Here $b_{\min} \ll b \ll R_G$ is a cutoff value for the impact parameter, and we have defined

$$I_n(x_{\min}) \equiv \int_{-1}^{+1} dz \int_{x_{\min}}^{\sqrt{1-z^2}} \frac{dx}{x(x^2+z^2)^{n/2}} . \tag{7}$$

This quantity diverges only logarithmically for $x_{\min} \to 0$. For example, one easily finds that $I_1(x_{\min}) \approx (\ln x_{\min})^2 - 2\ln 2 \ln x_{\min}$, so that $I_1 \lesssim 100$ for a wide range of $10^{-4} < x_{\min} < 10^{-1}$.

Similarly, the red giant's core receives a velocity increment

$$|\delta v_{\rm core}(x)| = \frac{2Gm_c}{v_r b} , \tag{8}$$

corresponding to a change in energy

$$\Delta E_{\rm core} = \frac{2G^2 m_{\rm core}^3}{v_r{}^2 b^2} . \tag{9}$$

Depending on whether or not $\Delta E_{\rm core}$ is larger than the binding energy of the red giant's core to its envelope, the core may or may not escape (cases 1 and 2 of § II*a*). This was the basis of the analysis presented by Tuchman (1985).

When v_r becomes smaller than a certain critical value $[v_r^{\rm crit}/\tilde v \sim (m_{\rm core}/m_G)^{1/2} \times (R_G/b)^{1/2}]$, it is no longer justified to treat the motion of the core in the impulsive approximation. However, the energy dissipated in the envelope, which reacts on a somewhat longer time scale than the core, can still be approximated by equation (6). In this case, the core may get captured by the passing compact star, so that they emerge together as a binary.

The maximum relative velocity $v_r^{\max}$ for binary formation at

[3] Note that the original calculation of Press and Teukolsky (1977) contained a numerical error which was corrected in later papers (see Lee and Ostriker 1986; Giersz 1986; McMillan, McDermott, and Taam 1987).

small impact parameters can be approximately evaluated by setting $\Delta E_{\rm env} = \mu (v_r^{\rm max})^2/2$, where μ is the reduced mass. This gives

$$\frac{v_r^{\rm max}}{\tilde{v}} = \left[2(3-n)\left(1+\frac{m_c}{m_G}\right)\left(\frac{m_c}{m_G}\right)\left(\frac{m_{\rm env}}{m_G}\right)I_n\right]^{1/4} . \quad (10)$$

Alternatively, if we take the relative velocity at infinity $v_r = 0$, we may use equation (6), with v_r replaced by the periastron velocity v_p, to estimate how tightly a binary can be bound by a head-on collision. To do this, we make the assumption that all the energy tidally dissipated in the envelope is converted into binding energy for the emerging binary. Specifically, we can evaluate the minimum semimajor axis $a_{\rm min}$ of the binary by setting $\Delta E_{\rm env} = G m_{\rm core} m_c/2a_{\rm min}$. This gives

$$\frac{a_{\rm min}}{R_G} = \left(\frac{m_{\rm core}}{m_{\rm env}}\right)\left(\frac{m_G}{m_c}\right)\left(\frac{1}{2(3-n)I_n}\right)\left(\frac{v_p^2}{\tilde{v}^2}\right) . \quad (11)$$

Given the typical values of I_n, it is easy to see that, for $m_c/m_G \sim 1$, this can give at best $a_{\rm min}/R_G \sim 10^{-2}$.

c) Estimating Capture Cross Sections and Formation Rates

In general, the capture cross section $\pi b_{\rm max}^2(v_r)$ of a compact star by a red giant must be determined numerically by simulating a large number of encounters with varying relative velocities and impact parameters. Once this has been done, specific formation rates may be evaluated by integrating over the relevant parameters defining the environment in which the encounters are taking place. In particular, for a single mass ratio (otherwise the rates computed for each mass bin would simply be added together), the formation rate per unit volume can be calculated as

$$\Gamma = n_c n_G \int [\pi b_{\rm max}^2(v_r)] v_r f(\mathbf{v}_r) d^3\mathbf{v}_r , \quad (12)$$

where n_c and n_G are the number densities of, respectively, neutron stars and red giants, and f is the distribution of relative velocities. If both neutron stars and red giants can be described by Maxwellian velocity distributions with velocity dispersion σ, then

$$f(\mathbf{v}_r) d^3\mathbf{v}_r = \frac{1}{2\sqrt{\pi}\sigma^3} \exp\left(-\frac{v_r^2}{4\sigma^2}\right) v_r^2 \, dv_r . \quad (13)$$

In this case, we can compute the rate, from equations (12) and (13), as

$$\Gamma \equiv n_c n_G R_G^2 \tilde{v}\Omega = 0.005\left(\frac{n_c}{10^2\ {\rm pc}^{-3}}\right)\left(\frac{n_G}{10^3\ {\rm pc}^{-3}}\right) \times \left(\frac{R_G}{10^2\ R_\odot}\right)^2\left(\frac{\tilde{v}}{10\ {\rm km\ s}^{-1}}\right)\Omega \times 10^{-9}\ {\rm yr}^{-1}\ {\rm pc}^{-3} . \quad (14)$$

Here we have defined a new quantity Ω, representing the nondimensional overlap integral between the flux $v_r f(v_r)$ and the cross section $\pi b_{\rm max}^2(v_r)$, according to equations (12) and (14).

Alternatively, we can compare equation (14) to the rate of binary formation by tidal capture of neutron stars by main-sequence stars, written in a similar way as $\Gamma_{\rm ms} = n_c n_{\rm ms}[\pi (b_{\rm max}^{\rm ms})^2]\sigma$, where $b_{\rm max}^{\rm ms}$ is the maximum impact parameter for tidal capture of a neutron star by a main-sequence star and $n_{\rm ms}$ is the number density of main-sequence stars. From equation (14), we see that

$$\frac{\Gamma}{\Gamma_{\rm ms}} = \left(\frac{\tilde{v}}{\sigma}\right)\left(\frac{n_G}{n_{\rm ms}}\right)\frac{\Omega R_G^2}{\pi (b_{\rm max}^{\rm ms})^2} . \quad (15)$$

The quantity Ω, in equations (14) and (15), depends only on the nondimensional ratio $\sigma/\tilde{v}$ of the velocity dispersion in the system to the characteristic internal velocity of an encounter. This ratio, together with n_c and n_G, completely characterizes the environment from the point of view of calculating rates. Figure 1 illustrates qualitatively two extreme combinations of relative velocity distribution and capture cross section. When the velocity dispersion in the cluster is much smaller than the characteristic velocity $\tilde{v}$ (Fig. 1*a*), the binary formation rate is dominated by distant encounters, and $\Omega \gg 1$. It is in this case only that the capture cross section can be approximately evalu-

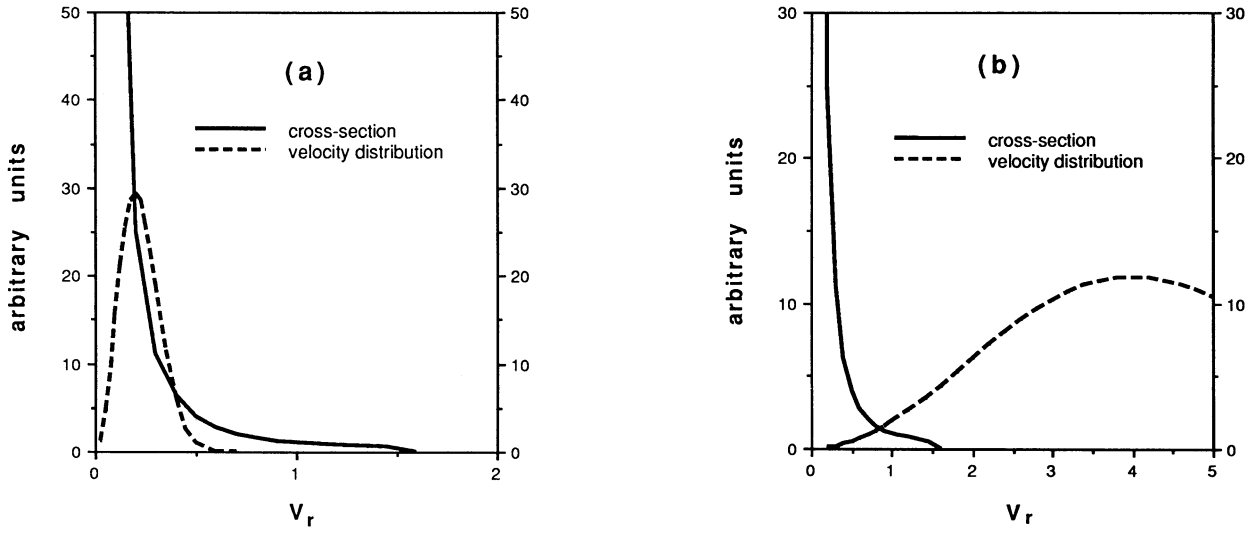

FIG. 1.—Competing contributions to the rate integral (eq. [12]). The figure illustrates qualitatively the fundamental importance of the ratio $\tilde{v}/\sigma$ of the characteristic velocity of an encounter, $\tilde{v}$ ($\approx$ envelope sound speed), to the velocity dispersion σ in the system. The solid line represents a typical cross section for binary formation, whereas the dashed line shows the distribution of relative velocities (eq. [13]). In (*a*), $\tilde{v}/\sigma \gg 1$ and binary formation is dominated by distant, tidal encounters between stars with relative velocities $v_r \approx \sigma$. In (*b*), $\tilde{v}/\sigma \ll 1$, and binary formation occurs only through direct collisions between stars with very low relative velocities.

ated using the tidal approximation. In the opposite case (Fig. 1*b*), when the velocity dispersion in the cluster is significantly larger than $\tilde{v}$, the formation rate is determined primarily by penetrating encounters taking place between stars in the low relative velocity valley of the distribution, and $\Omega \ll 1$.

For encounters with red giants (radii $R_G \gtrsim 100\ R_\odot$) in globular clusters, we will see in § III that an intermediate configuration is encountered, where the velocity dispersion $\sigma \approx \tilde{v}$, and $\Omega \lesssim 1$. For encounters with stars on the subgiant branch ($R_G \sim 10\ R_\odot$), the situation is close to that of Figure 1*a*. In the Galactic center, the velocity dispersion is about an order of magnitude larger, and the situation is very close to that of Figure 1*b*.

d) Probability Distributions for Other Observable Quantities

We now give the procedure we use to calculate the probability distributions for quantities such as the eccentricity or the semimajor axis of the binaries. These are easily computed once a sufficiently detailed exploration of the parameter space has been accomplished. Here again we assume a given mass ratio m_c/m_G for simplicity. The results are trivially generalized by superposing the distributions obtained for each mass bin.

For definiteness, let us consider the semimajor axes. The probability of forming a binary with a semimajor axis smaller than a given value a is computed as

$$P(<a) = \int\int_{\mathscr{D}<a} p(v_r, b) dv_r\, db\ , \tag{16}$$

where $p(v_r, b)$ is the probability of an encounter occurring with relative velocity at infinity v_r and impact parameter b. Up to a normalization factor, this quantity is simply the product of the relative velocity distribution, equation (13), with

$$p_{v_r}(b) = \begin{cases} 2b/b_{\rm crit}^2, & \text{for } b < b_{\rm crit}; \\ = 0, & \text{otherwise,} \end{cases} \tag{17}$$

where $b_{\rm crit} \gg R_G$ is a constant. The domain of integration, $\mathscr{D}_{<a}$, is the region of the (v_r, b) plane where the semimajor axes of the binaries are found to be less than the prescribed value. In order to determine the location of this region with any reasonable accuracy, a large number of representative points in this plane must be calculated.

The procedure is identical to obtain other distributions, such as that of the binary eccentricities or the envelope ejection velocities.

III. SOME PRELIMINARY NUMERICAL SIMULATIONS

We now describe a set of numerical simulations which we performed to provide preliminary answers to an otherwise very complicated problem. These simulations provide only very crude results for some aspects of the problem. However, they have the advantage of being fully three-dimensional, and they model the mass distributions, global gravitational dynamics, and internal energetics self-consistently and in a qualitatively reasonable fashion.

a) Red Giant Model and Numerical Techniques

In this section, all masses are expressed in units of the giant's mass m_G and all distances are in units of the giant's radius R_G. The natural unit of velocity for the problem is then

$$\tilde{v} \equiv \sqrt{\frac{Gm_G}{R_G}} = 44\ \text{km s}^{-1} \left(\frac{m_G}{1\ M_\odot}\right)^{1/2} \left(\frac{R_G}{10^2\ R_\odot}\right)^{-1/2}. \tag{18}$$

For all the simulations presented here, we adopt a generic red giant model consisting of a point mass core, with mass $m_{\rm core} = 0.6$, surrounded by an extended envelope of mass $m_{\rm env} = 0.4$. The density profile in the envelope is similar to that of the models presented by Tuchman, Sack, and Barkat (1978); i.e., we use the density profile of equation (1) with $n = 1$. For the mass of the compact object, also taken to be a point mass, we use $m_c = 1$ in most cases and $m_c = 0.2$ in a few special other examples as noted.

To model the dynamics of the encounter, we use a pseudo-particle method. The envelope of the giant is represented by a large number N of point particles, all of equal masses, with an initial distribution matching the density profile of our model. The particles evolve in time under the influence of their own self-gravity as well as the gravitational attraction to the core and to the compact star. "Pressure" is represented by giving the particles an isotropic velocity dispersion. At $t = 0$, initial positions and velocities for all particles are determined by sampling a continuous phase space distribution function. This distribution function is obtained self-consistently from the density profile and the assumption of isotropy by an inversion procedure borrowed from stellar dynamics (see, e.g., Binney and Tremaine 1987, p. 236 for a description).

The subsequent dynamical evolution of the system was computed numerically with a standard Aarseth N-body code (Aarseth 1985). Accordingly, we evolved a fluid system as if it were a collisionless gas. While this is not correct in detail, it does provide a reasonable, qualitative picture of the bulk mass motions and gravitational dynamics. All simulations were done with $N = 512$ particles representing the envelope, except for a few runs which were repeated with $N = 1024$ and $N = 2048$, in order to check that the results were reasonably insensitive to discrete particle effects.

b) Exploring the Parameter Space

The direct N-body code we used for these simulations does not allow us to use very large numbers of particles. For this reason, it has not been possible to reliably study cases in which the mass ratio m_c/m_G was much smaller than unity. This is because discrete particle effects become dominant in these cases, the gravitational encounters between the point mass perturber and individual particles in the envelope becoming more and more important as the mass m_c is decreased. On the other hand, in cases where the mass ratio is very small, say $m_c/m_G < 0.1$, the giant star's structure is only very weakly perturbed by the presence of the compact object. Other physical processes, occurring on a time scale much longer than the dynamical time scale, become important. These processes, such as secular angular momentum and heat transport in the envelope or turbulent viscosity (see Taam, Bodenheimer, and Ostriker 1978), are not properly treated by our simulations, and our results would therefore be meaningless for such cases.

Based on these considerations, we have chosen to set the mass ratio $m_c/m_G = 1$ in almost all cases. However, the entire ranges of possible values for the other two parameters were systematically covered. Specifically, the impact parameter b/R_G and the relative velocity $v_r/\tilde{v}$ were both varied from zero to large values greatly exceeding unity. In addition, we have studied just a few cases with $m_c/m_G = 0.2$, in order to determine, at least qualitatively, the influence of a reduced mass ratio.

Figures 2–5 show the results of simulations which illustrate most of the typical cases listed in § II*a*. All the figures have

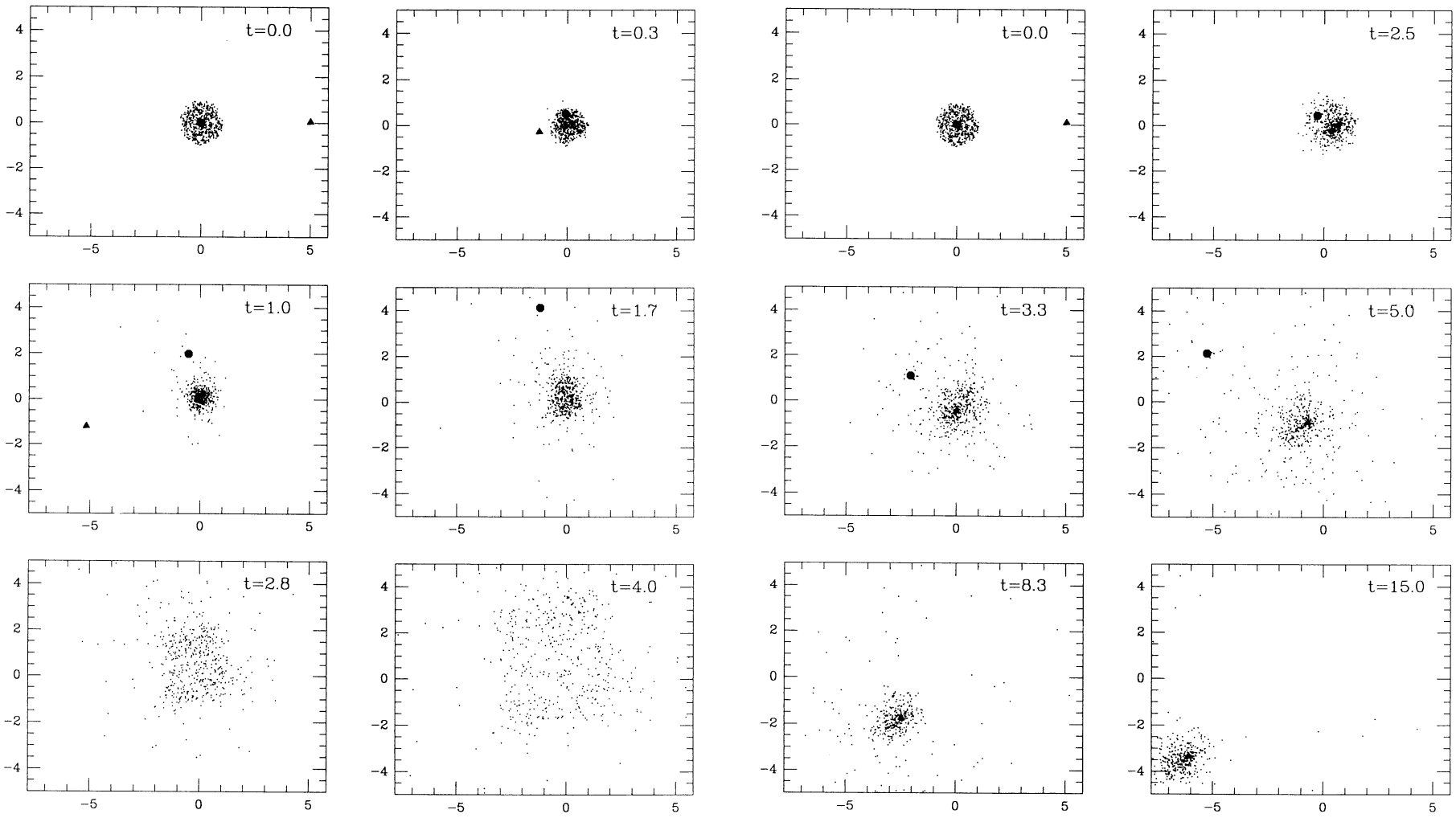

FIG. 2

FIG. 3

FIG. 2.—Typical encounter with core ejection followed by envelope disruption (case 2 of § II*a*). A projection onto the orbital plane is shown, with distances in units of R_G. The compact object is represented by the triangle, the red giant's core is represented by the heavy filled dot, and the red giant's envelope is represented by the small dots. At $t = 0$, the red giant is at rest at the origin and the compact object is moving toward the left. See text for discussion.

FIG. 3.—Exchange interaction (case 3 of § II*a*). Conventions are as in Fig. 2.

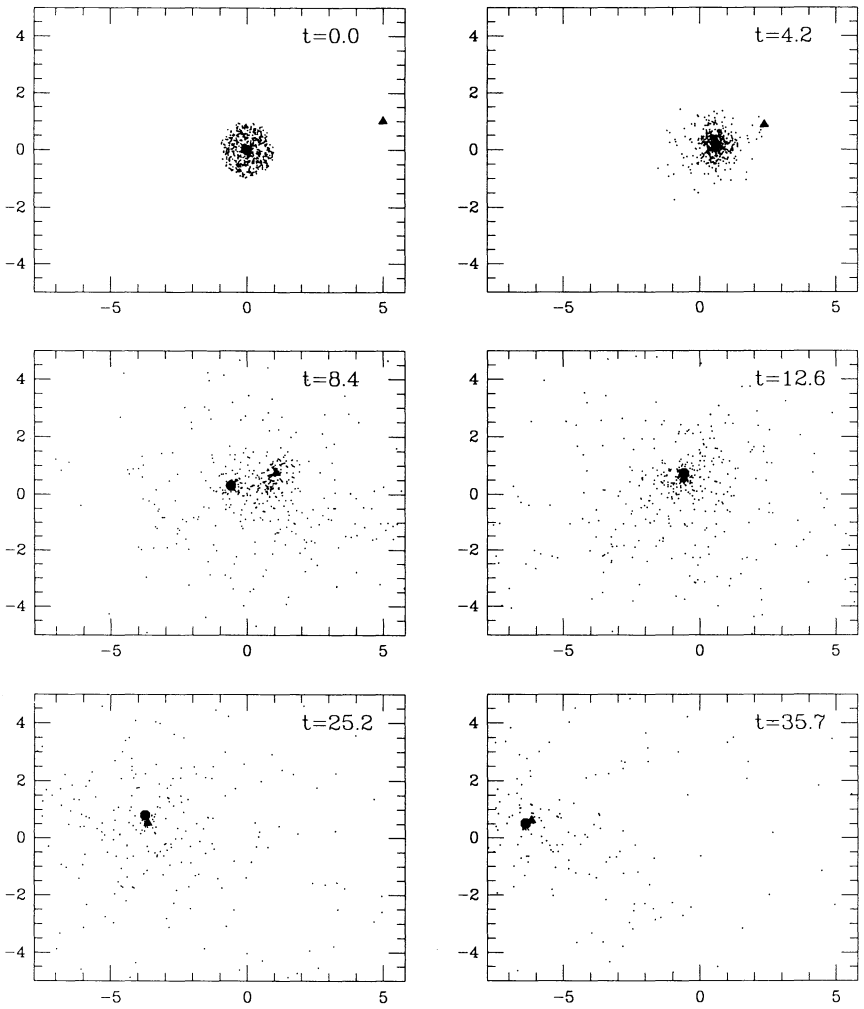

FIG. 4

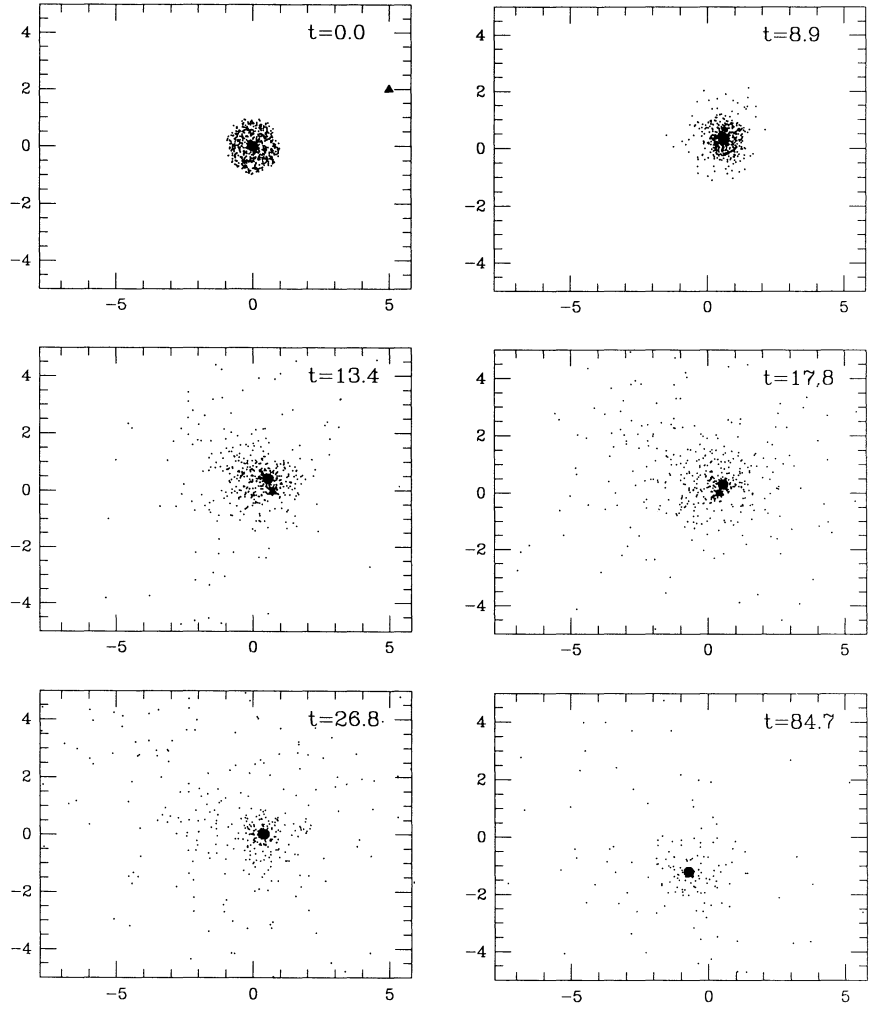

FIG. 5

FIG. 4.—Binary formation with dissipation of the envelope (case 4 of § II*a*). Conventions are as in Fig. 2. Note the rapid evolution, leading to a binary which retains a large eccentricity.
FIG. 5.—Typical encounter with smaller mass ratio: $m_c/m_G = 0.2$ (similar to case 5 of § II*a*). Conventions are as in Fig. 2.

been obtained with 512 particles and show a projection of the system onto the orbital plane. Coordinates along both axes are in units of the stellar radius R_G. The time is in units of the typical orbital time ($\approx$ envelope sound travel time) $t_0 \equiv$ 1982; Bieging 1984; Harvey, Lester, and Joy 1987; Mezger *et* red giant is at rest at the origin, whereas the compact star is at the point $x = 5$, $y = b$, moving in the $-x$ direction with velocity $v_x = -v_r$. The mass ratio is equal to unity everywhere except in Figure 5, which specifically illustrates a case with $m_c/m_G < 1$.

Core ejection, followed by envelope disruption (case 2 of § II*a*), is shown in Figure 2, which corresponds to $b/R_G = 0.05$ and $v_r/\tilde{v} = 15.0$. Note the strong hierarchy of time scales. The compact star moves across the envelope in the shortest time scale, followed by the slower escape of the core from the envelope. Finally, on the longest time scale, the envelope explodes. The explosion is slightly anisotropic, with principal axes clearly aligned along the trajectories of the core and compact object.

Figure 3 demonstrates the possibility of having an exchange interaction (case 3 of § II*a*), where the compact star takes the place of the red giant's core. This case was obtained with $b/R_G = 0.1$ and $v_r/\tilde{v} = 3.0$. Following the primary interaction, the core escapes, accreting a small amount of mass, but the compact star subsequently remains trapped inside the potential well of the (slightly perturbed) envelope.

A typical case of binary formation, corresponding to case 5 of § II*a*, is illustrated in Figure 4, obtained with $b/R_G = 1.0$ and $v_r/\tilde{v} = 0.8$. Note how the envelope is immediately disrupted in just a few crossing times. Clearly, the energy is very quickly dissipated here, and there is nothing like a "slow spiral-in." The binary later moves along with the remnant low-density cloud, accreting some of the gas. At the end of the integration, the binary has stabilized into an orbit with semimajor axis $a = 0.21$ and eccentricity $e = 0.29$.

Finally, Figure 5 shows another case of binary formation, similar to that of Figure 4, but where the mass ratio $m_c/m_G =$ 0.2. The other two parameters have the same values as in Figure 4. Here the ejection of the envelope is completed only after a much larger number of orbital times (as in case 5 of § II*a* above). By the end of the integration, the binary has a semimajor axis $a = 0.08$ and eccentricity $e = 0.11$.

c) *Binary Formation*

Figure 6 shows the maximum impact parameter $b_{\max}$ for binary formation, as a function of the relative velocity at infinity v_r, for $m_c/m_G = 1$. Each point of the curve must come from a series of runs aimed at determining the critical impact parameter $b_{\max}$ beyond which no bound system is formed. The large impact parameter behavior appears to be rather well described by the approximate analytic expression of equation (4). This should not be too surprising here, since equation (4) is expected to apply best to the stellar dynamical case. The maximum impact parameter goes to zero at a critical velocity $v_r/\tilde{v} = 1.6$. This is in reasonable agreement with the analytical estimate of equation (10), which predicts $v_r^{\max} \approx 2$–4 for $n = 1$ and $I_1 \approx$ 10–100.

Most importantly, we find that a relative velocity $v_r \approx \tilde{v}$ separates binary-forming penetrating encounters ($b_{\max}/R_G < 1$) from distant encounters ($b_{\max}/R_G > 1$). Typical velocity dispersions in the cores of globular clusters are comparable to the value of $\tilde{v}$ for stars on the red giant branch (see eq. [18] above). Accordingly, for these stars the situation is somewhat intermediate between those illustrated in Figure 1*a* and Figure 1*b*, and rate calculations should take into account both penetrating and distant encounters. A numerical estimate of Ω in equation (14), based on the cross section from Figure 6 (eq. [4] was used to extrapolate for $v_r \to 0$) and the relative velocity distribution of equation (13) with $\sigma = \tilde{v}$, gives $\Omega \approx 0.2$.

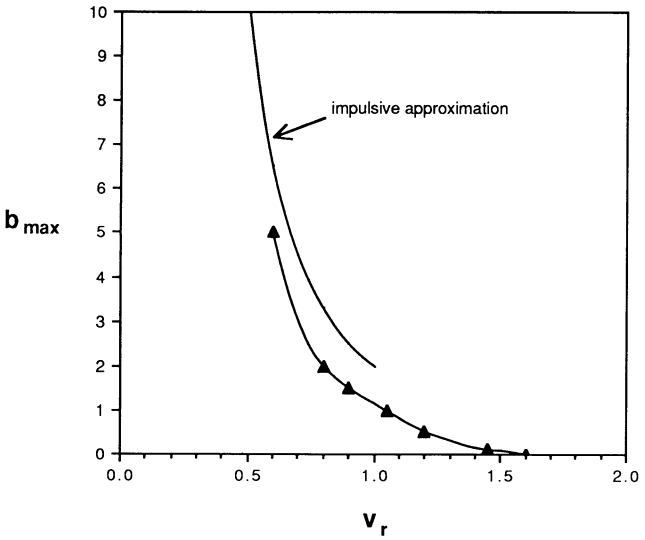

FIG. 6.—Maximum impact parameter for binary formation, as determined by our numerical simulations (for the case $m_c/m_G = 1$) and comparison to the impulsive approximation. Here $b_{\max}$ is in units of the red giant's radius R_G and the relative velocity at infinity, v_r, is in units of $\tilde{v}$ (eq. [18]).

For stars on the subgiant branch, the ratio $\tilde{v}/\sigma \gg 1$, and we are in the situation of Figure 1*a*, where we expect that the tidal approximation should apply. Repeating the same calculation as above for $\tilde{v}/\sigma = 10$, we find that $\Omega \approx 500$ in this case. For the ratio of number densities we take $n_G/n_{\rm ms} \approx 10^{-2}$ (see Verbunt 1988*a*, Table 5),[4] whereas the results of calculations for the tidal capture by main-sequence stars indicate $(R_G/b_{\max}^{\rm ms})^2 \sim 10^{-3}$ for $R_G \sim 10\ R_\odot$ (see, e.g., Lee and Ostriker 1986, in particular their eq. [2.10]). By equation (15), we then obtain a relative rate of binary formation $\Gamma/\Gamma_{\rm ms} \approx 0.05$. This is indeed in good agreement with the results of Verbunt (1988*b*), based on the tidal approximation.

The semimajor axes and eccentricities of the resulting binaries, as a function of the encounter parameters, are shown in Figures 7 and 8. Along any sequence with fixed impact parameter b, the semimajor axis (Fig. 7) first remains very close to its minimum value at $v_r = 0$, and then rather suddenly increases to infinity as v_r approaches the critical value $v_r^{\rm crit}(b)$ beyond which no bound system is formed. Along the same sequence, the eccentricity (Fig. 8) has a local minimum for some intermediate value $0 < v_r < v_r^{\rm crit}(b)$, and, as expected, goes to unity at both ends of the sequence. The absolute minimum appears to be realized along the sequence corresponding to grazing incidence ($b \approx 1$).

It is clear from Figures 7 and 8 that most of the binaries that are formed have rather large eccentricities ($e > 0.2$) and semimajor axes $a \sim 0.1\ R_G$. The procedure of § II*d* for calculating the probability distributions of a and e is only marginally applicable here, given the crudeness of the numerical method

[4] This number ignores mass segregation in the cluster, which may significantly increase the importance of captures by giants; see Verbunt and Meylan (1989).

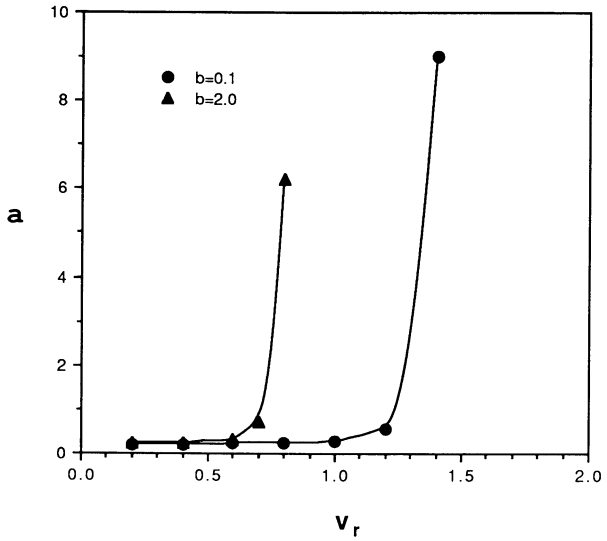

FIG. 7.—Semimajor axes a of the binaries formed along two constant impact parameter sequences. Units are as in Fig. 6. The semimajor axes along each sequence first remain very close to the minimum value at $v_r = 0$, and then rather suddenly increase to infinity as the relative velocity approaches a critical value beyond which no binary is formed.

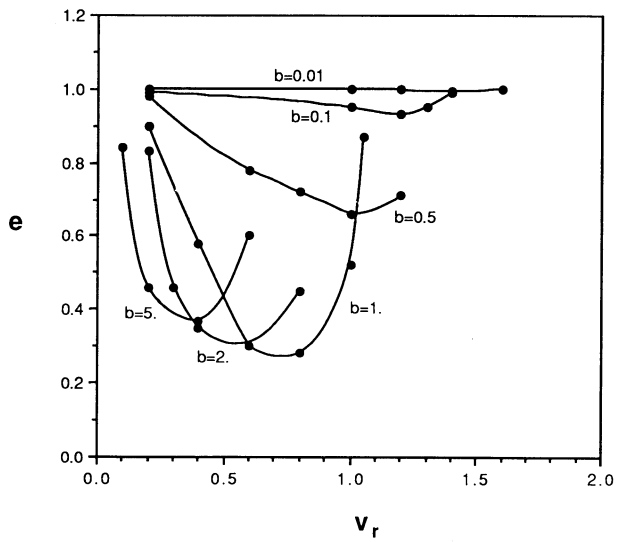

FIG. 8.—Eccentricities e of the binaries formed along several constant impact parameter sequences. Units are as in Fig. 6. The eccentricity goes to unity at both ends of each sequence, as expected, and present a local minimum somewhere in between. The absolute minimum appears to be realized along the sequence corresponding to grazing incidence ($b/R_G \approx 1$).

and the relatively coarse coverage of the (v_r, b) plane. We use a two-dimensional trapezoidal rule to carry out the integration in equation (16) for each value of a. We first fix the impact parameter b, and integrate with respect to v_r, from zero to some value $v_{r_2}(b)$ beyond which a becomes larger than the prescribed value [see Fig. 7; we determine $v_{r_2}(b)$ by linear interpolation between the two nearest known points along the sequence]. The integration with respect to b is carried out last, with b varying from zero to a large constant value, here $b = 5R_G$ (using the analytic expression from eqs. [3]–[4], one can verify that the contribution from even larger impact parameters is negligible). The procedure for the eccentricity is identical, except that now two boundary points $v_{r_1}(b)$ and $v_{r_2}(b)$ have to be determined by interpolation, such that the eccentricity along the sequence is less than e when $v_{r_1}(b) < v_r < v_{r_2}(b)$ (see Fig. 8). When carried out in this fashion, the procedure indicates the most probable values $a \approx 0.15R_G$ and $e \approx 0.6$ when $\sigma = \tilde{v}$. These values are only slightly reduced by decreasing the mass ratio to $m_c/m_G = 0.2$. When $\sigma/\tilde{v} < 1$, the most probable value of a remains virtually unchanged, while that of the eccentricity increases slightly.

IV. DISCUSSION

Only very few binary sources in globular clusters have been directly observed (Table 1). The large disparity in the values of their orbital elements makes it very difficult to define what we expect to be the properties of a typical binary. However, from the results of § III, it appears quite possible that at least the binaries with small separation but large eccentricity, such as those recently reported in 47 Tuc and M15, may directly result from a recent encounter of a neutron star with a subgiant branch star. Indeed, contrary to widespread belief, such an encounter *typically does not lead to a "slow spiral-in" and circularization of the orbit.* Instead, the energy dissipation occurs rapidly, in just a few orbital times, and the binary retains a large eccentricity.

Naturally the ages of the binaries listed in Table 1 are not known, and one could imagine that they were born through a red giant/neutron star encounter but later evolved into what we observe today. In particular, for the ultracompact X-ray binary 4U 1820−30, one possible evolutionary scenario has been constructed which would imply an age greater than 10^9 yr

TABLE 1

KNOWN BINARIES IN GLOBULAR CLUSTERS

Source	Type	P_{orb}	a ($R_\odot$)[a]	e
X 2127+119 (M15)[b]	LMBX	8.5 hr	2	?
4U 1820−303 (NGC 6624)[b]	LMBX	11 minutes	0.15	?
PSR 1620−26 (M4)[c]	Binary pulsar (P = 11 ms)	195 days	140	0.025
PSR 0021−72 A (47 Tuc)[d]	Binary pulsar (P = 4.5 ms)	33 minutes	0.3	0.3
PSR 2127+11 C (M15)[e]	Binary pulsar (P = 30 ms)	8.2 hr	2	? (large)

[a] From P_{orb} and Kepler's law with $M_{tot} = 1\ M_\odot$.
[b] See, e.g., Parmar and White 1988.
[c] Lyne *et al.* 1988; McKenna and Lyne 1988.
[d] Ables *et al.* 1988.
[e] Anderson *et al.* 1989; Wolszczan 1989.

(Rappaport *et al.* 1987). This would also imply that the binary might have formed at an early epoch in the history of NGC 6624, when the masses of the red giants could still have been $\gg 1\ M_\odot$. While they may be essential in explaining the currently observed properties of the binaries, such evolutionary scenarios are, however, beyond the scope of this paper.

Some of the binaries formed by red giant/neutron star encounters may also contribute very significantly to the heating of a globular cluster during its late stages of evolution (see McMillan, McDermott, and Taam 1987). Let us define the hardness χ of a binary as the ratio of its binding energy to the mean kinetic energy of a typical star with mass m,

$$\chi \equiv \frac{(Gm_c\, m_{\rm core}/2a}{\frac{1}{3}m\sigma^2} \approx 30\left(\frac{a}{10^2\ R_\odot}\right)^{-1}\left(\frac{m}{1\ M_\odot}\right)\left(\frac{\sigma}{10\ {\rm km\ s^{-1}}}\right)^{-2}. \tag{19}$$

In the final expression, we have set $m_c = m_{\rm core} = m$ for simplicity. Clearly, the binaries formed by red giant/compact star encounters are *hard* binaries, i.e., they have $\chi > 1$. Therefore, they will not be disrupted by subsequent interactions with other stars in the cluster. However, their hardness may also be small enough that their probability of being ejected from the cluster by interacting with a third star is very low (only when $\chi \gtrsim 25$ would this cease to be true). This will be the case at least for the binaries resulting from encounters with stars near the tip of the red giant branch (which give $a \gtrsim 100\ R_\odot$). In fact, for these binaries, the hardness may very well be in the range $5 < \chi < 10$, where they will contribute most strongly to cluster heating (Giannone and Molteni 1985).

From a more fundamental point of view, the very approximate calculations presented in this paper have not allowed us to present a very accurate description of an individual encounter. In particular, the hydrodynamics of the envelope has not been correctly modeled. To do so requires three-dimensional hydrodynamical calculations, which until very recently have been beyond the capabilities of computers. In a forthcoming publication, however, we will repeat our calculations using the SPH technique ("smooth particle hydrodynamics"). This technique has been successfully used recently to study several other types of three-dimensional stellar interactions (Benz and Hills 1987; Evans and Kochanek 1989) and should prove useful here.

We are very grateful to D. Chernoff for providing us with his own version of an Aarseth N-body code. It is a pleasure to thank the referee for several helpful suggestions for improving the manuscript. This work has been supported by National Science Foundation grants AST 87-14475 and PHY 86-03284 to Cornell University. Fellowship support from the John Simon Guggenheim Memorial Foundation is also gratefully acknowledged by S. L. S. Computations were performed on the Cornell National Supercomputer Facility, which is supported in part by the National Science Foundation, IBM Corporation, New York State, and the Cornell Research Institute.

REFERENCES

Aarseth, S. J. 1985, in *Multiple Time Scales*, ed. J. U. Brackbill and B. I. Cohen (Orlando: Academic Press), p. 377.
Ables, J., Jacka, C. E., McConnel, D., Hamilton, P. A., McCulloch, P. M., Hall, P. J. 1988, *IAU Circ.*, No. 4602.
Anderson, S., Gorham, P., Kulkarni, S., Prince, T., and Wolszczan, A. 1989, *IAU Circ.*, No. 4772.
Bailyn, C. D. 1988, *Nature*, **332**, 330.
Benz, W., and Hills, J. G. 1987, *Ap. J.*, **323**, 614.
Binney, J., and Tremaine, S. 1987, *Galactic Dynamics* (Princeton: Princeton University Press).
Bodenheimer, P., and Taam, R. E. 1984, *Ap. J.*, **280**, 771.
Evans, C. R., and Kochanek, C. S. 1989, *Ap. J. (Letters)*, **346**, L13.
Fabian, A. C., Pringle, J. E., and Rees, M. J. 1975, *M.N.R.A.S.*, **172**, 15P.
Giannone, G., and Molteni, D. 1985 in *IAU Symposium 113, Dynamics of Star Clusters*, ed. J. Goodman and P. Hut (Dordrecht: Reidel), p. 321.
Giersz, M. 1986, *Acta Astr.*, **36**, 181.
Lacy, J. H., Townes, C. H., Geballe, T. R., and Hollenbach, D. J. 1980, *Ap. J.*, **241**, 132.
Lacy, J. H., Townes, C. H., and Hollenbach, D. J. 1982, *Ap. J.*, **262**, 120.
Lee, H. M., and Ostriker, J. P. 1986, *Ap. J.*, **310**, 176.
Livio, M., and Soker, N. 1988, *Ap. J.*, **329**, 764.
Livne, E., and Tuchman, Y. 1988, *Ap. J.*, **332**, 271.
Lyne, A. G., Biggs, J. D., Brinklow, A., Ashworth, M., and McKenna, J. 1988, *Nature*, **332**, 45.
McKenna, J., and Lyne, A. G. 1988, *Nature*, **336**, 226.
McMillan, S. L. W., McDermott, P. N., and Taam, R. E. 1987, *Ap. J.*, **318**, 261.
Parmar, A. N., and White, N. E. 1988, *Mem. Soc. Astr. Italiana*, **59**, 147.
Press, W. H., and Teukolsky, S. A. 1977, *Ap. J.*, **213**, 183.
Rappaport, S., Nelson, L. A., Ma, C. P., and Joss, P. C. 1987, *Ap. J.*, **322**, 842.
Rasio, F. A., and Shapiro, S. L. 1990, in preparation.
Spitzer, L. 1987, *Dynamical Evolution of Globular Clusters* (Princeton: Princeton University Press).
Sutantyo, W. 1975, *Astr. Ap.*, **44**, 227.
Taam, R. E., Bodenheimer, P., and Ostriker, J. P. 1978, *Ap. J.*, **222**, 269.
Tuchman, Y. 1985, *Ap. J.*, **288**, 248.
Tuchman, Y., Sack, N., and Barkat, Z. 1978, *Ap. J.*, **219**, 183.
Verbunt, F. 1987, *Ap. J. (Letters)*, **312**, L23.
———. 1988*a*, in *Neutron Stars: Their Birth, Evolution, Radiation and Winds*, ed. W. Kundt (Dordrecht: Kluwer), in press.
———. 1988*b*, in *Timing Neutron Stars*, ed. H. Ögelman and E. P. J. van den Heuvel (Dordrecht: Kluwer), p. 593.
Verbunt, F., and Meylan, G. 1989, *Astr. Ap.*, **203**, 297.
Wijers, R. A. M. J. 1989, *Astr. Ap.*, **209**, L1.
Wolszczan, A. 1989, private communication.

FREDERIC A. RASIO and STUART L. SHAPIRO: Cornell University, Space Sciences Building, Ithaca, NY 14853